社団法人　電子情報通信学会
THE INSTITUTE OF ELECTRONICS,
INFORMATION AND COMMUNICATION ENGINEERS

信学技報
TECHNICAL REPORT OF IEICE.

エピポーラ平面画像解析に基づいた路上駐車車両の検出

朱　成華†　　平原　清隆†　　池内　克史†

† 東京大学生産技術研究所
〒 153-8505 東京都目黒区駒場 4-6-1
E-mail: †{zhu,hirahara}@cvl.iis.u-tokyo.ac.jp

あらまし　路上駐車車両は交通渋滞，交通事故などの原因となり，路上駐車の実態を把握することは，効果的な道路交通施策を考える上で重要である．従来，路上駐車車両の計測は計測車両に同乗した調査員による手動計測で行われていた．私たちは路上駐車車両を自動検出するシステムを提案する．検出用センサとしてコストの低いカメラを用いる．エッジ法と領域法の融合アルゴリズムによって，ラインスキャンカメラで得られたエピポーラ平面画像上の奥行き情報とテクスチャ情報から駐車車両を検出する．実環境での融合アルゴリズムの検出率は 96%に達した．

キーワード　エピポーラ平面画像，路上駐車車両，ラインスキャンカメラ，　特徴軌跡，　領域分割，モルフォロジー，テンプレートマッチング

Street-Parking Vehicle Detection Based on EPI Analysis

Cheng HUA ZHU†, Kiyotaka HIRAHARA†, and Katsushi IKEUCHI†

† Institute of Industrial Science, University of Tokyo
4-6-1, Komaba, Meguro-ku, Tokyo, 153-8505 Japan
E-mail: †{zhu,hirahara}@cvl.iis.u-tokyo.ac.jp

Abstract　Street-parking vehicles cause traffic congestions and accidents. It is very important for traffic census to obtain the number of those vehicles. At present, street-parking vehicles are counted manually by investigaters. We use a camera sensor for detecting street-parking vehicles because of its low cost. We proposed an automatic detection method for street-parking vehicles. The method is based on an epipolar-plane image (EPI) analysis. EPIs include depth information between objects and the camera and texture information shown in the vehicles bodies. Both informations are calculated by fusing edge- and region-based algorithms. As a result of experiments in roads, a detection rate reached 96%.

Key words　Epipolar-Plane Image, Street-Parking Vehicle, Line Scan Camera, Feature Path, Region Segmentation, Morphology, Template Matching

1. Introduction

Street-parking vehicles reduce amount of traffic flows in streets and interfere with drivers view, resulting in traffic congestions and accidents. Proper traffic management requires grasping the number of parking vehicles along streets. Currently, manual methods are employed to count such numbers. In order to increase the efficiency of traffic managements, we propose a method to automatically count the number of parking vehicles.

There are two kinds of sensors for detecting vehicles. The first one is an active sensor, such as laser range sensor which have high accuracy for vehicle detection. Related work was performed by Ono [1], et al. They used a scanning laser sensor and obtained the distance to the targeted street-parking vehicles directly.

Another kind of sensors are passive sensors, such as camera sensors. They have some vulnerability to drastic changes in outdoor environment, however, such detailed information as texture of objects can be obtained. It is useful for vehicle classification and so on.

This paper describes two methods to detect street-parking vehicles from an EPI (Epipolar-Plane Image) generated by a line scan camera: an edge-based method and a region-based method. The first method is based on EPI analysis [2] [3] [4], a technique for building a three-dimensional description of a

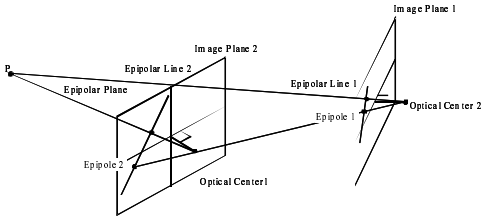

図 1　2 台のカメラによるステレオ構成
Fig. 1　Stereo configuration with two cameras

static scene from a dense sequence of images. EPI analysis is used to calculate the features depth from the slope of feature paths in EPIs. The other method is based on a region segmentation of EPIs. Vehicle regions and background regions can separated using region segmentation of EPI.

This paper is organized as follows. In section 2, we introduce an EPI generation. Section 3 describes edge-based method. Section 4 describes region-based method. Section 5 describes the fusion of two methods. Section 6 presents results of experiments. Section 7 concludes this paper.

2. EPI Analysis and Feature Path

In this section, we introduce an EPI which can be generated by lateral motion of an image sensor. An EPI includes 3D and texture information in the original scene. We provide the outline of how to apply an EPI analysis to the detection of street-parking vehicles.

2.1 Epipolar-Plane Image

Fig.1 illustrates a general stereo configuration. Two cameras are modeled as pinholes with its optical centers, its image planes in front of its lenses, and a feature point P in a 3D scene. An epipolar plane is generated from the feature point P and the two optical centers. All the points in the epipolar plane are projected on epipolar lines in the image planes. An epipole is the intersection of an image plane with the line joining the optical centers. The epipolar plane contains all epipolar lines. An image constructed from this sequence of epipolar lines is called an epipolar-plane image (EPI). Similarly, an EPI can be also generated from the sequence of the images captured by only one camera. While the moving direction of its optical center is perpendicular to the camera orientation, the EPI is generated from the feature point P and the locus of the optical center (see Fig.2). This motion of the camera is called lateral motion. In lateral motion, all the epipolar lines in the image planes are the same straight line which is parallel to the locus of the optical center.

2.2 Feature Point and Feature Path

In an EPI generated by lateral motion, feature point, P draws a line, referred to as a feature path (see Fig.3). Under the assumption of lateral motion at a constant speed, feature paths are straight lines.

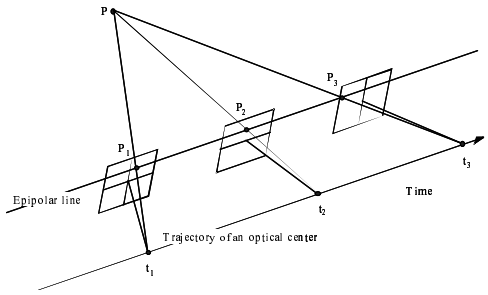

図 2　ラテラルモーションによる EPI の構築
Fig. 2　EPI generation from lateral motion

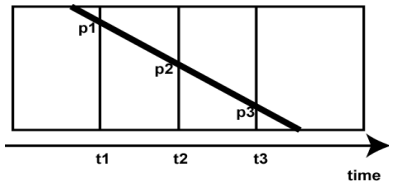

図 3　EPI 上の特徴軌跡
Fig. 3　Feature path on EPI

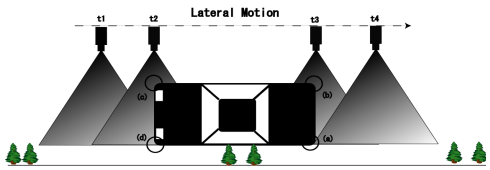

(a) Measuring method of street-parking vehicles

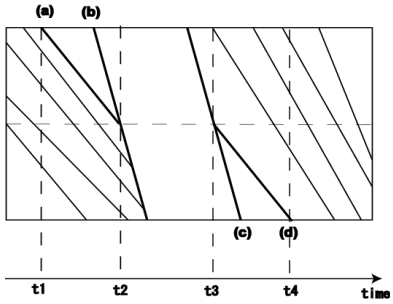

(b) Generated EPI

図 4　計 測 方 法
Fig. 4　Measuring method

The distances from the optical center to the image plane and the feature point are correspondingly indicated by h and D. The moving speed V of the optical center is constant. The slope m of the feature path on the EPI, is in proportion to D.

$$D = h \times V \times m$$

2.3 Feature Path of Street-Parking Vehicles

If the scanning lines are parallel to the locus of the camera movement (see Fig.2), EPI can be created by collecting one scan line in the time direction. Therefore, it is sufficient to

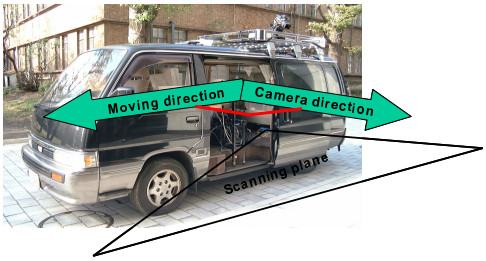

図 5　ラインスキャンカメラと計測車両
Fig. 5　Line scan camera and measurement vehicle

use a 1-dimentional CCD sensor instead of a 2-dimentional CCD sensor, and a line scan camera can generate an EPI. One of the advantages of a line scan camera is its very high frequency, which is around several kHz. Thus, the EPI is constituted in time direction and every feature path on the EPI is very smooth. In the method proposed for detecting street-parking vehicles, a line scan camera is mounted on a measurement vehicle and lateral motion is realized. Our system requires the scanning plane of the camera to be always kept horizontal and at as height as it can intersect the side body of street-parking vehicles. Fig.4 depicts the outline of the measuring method and a feature path in an EPI. We can detect the existence of street-parking vehicles from the following informations obtained by the feature paths in an EPI:

- Depth information

The distance D between the camera and a feature point can be determined from the slope of the corresponding feature path on an EPI. Street-parking vehicles are detected from the differences of the feature path (a) and (d),(b) and (c).

- Texture information

Because there is a few features in the body of vehicles, we can detect the street-parking vehicles from the feature's numbers. That is to say, we can also detect the street-parking vehicles from the number of feature paths on the EPI.

2.4　Acquisition of EPI

The line scan camera is oriented toward street-parking vehicles and perpendicular to the moving direction (see Fig.5).

The scanning plane becomes a horizontal plane. The measurement vehicle runs at constant speed, along a traffic lane. A scanning plane will be an epipolar plane and feature points on the scanning plane will draw the feature paths on the EPI.

3.　Edge-Based Method

As shown in the block diagram of Fig.6, our edge-based method for detecting street-parking vehicles analyzes depth variation (slope-angle curve) obtaining from EPI processing.

3.1　Creating of Slope-Angle Curve

An EPI processing consists of four main steps: (1) Image division, (2) edge detection, (3) line extraction, (4) plotting

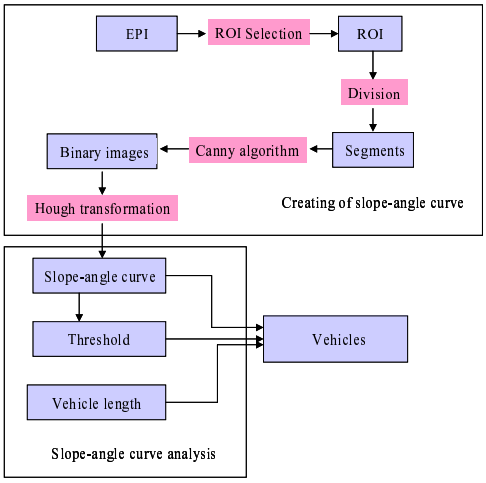

図 6　エッジ法のブロックダイアグラム
Fig. 6　Block diagram of edge-based method

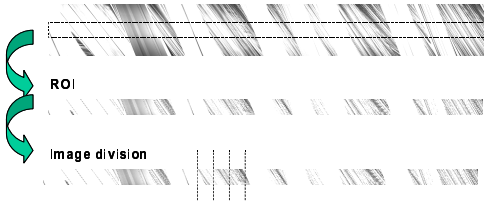

図 7　ROI と画像分割
Fig. 7　ROI and image division

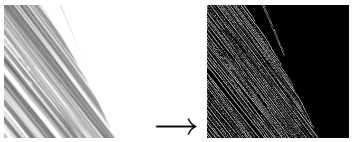

(a) stripe　　(b) Edge image

図 8　エッジ検出
Fig. 8　Edge detection

slope-angle curve. The processing method is described in this section.

3.1.1　Image Division

The depth between objects and the camera changes with the movement of the measurement vehicle. The slope of the feature path is varied according to the depth. The process for getting the slope variation first divides ROI into stripes with equal length (in time axis).

3.1.2　Edge Detection

We adopt Canny edge detector [5] for extracting edges in each stripes. Fig.8 shows an example of the result from Canny edge detector.

3.1.3　Feature Path Extraction

The strongest feature path in each stripe is extracted using Hough transformation [6]. As shown in Fig.10, θ and r are the slope angle and the perpendicular distance of a

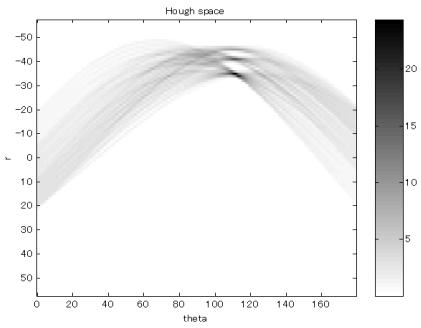

図 9　ハフ空間
Fig. 9　Hough space

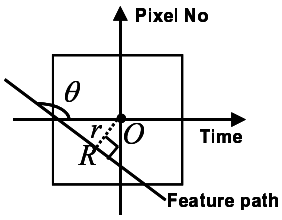

図 10　ハフ変換による特徴軌跡抽出
Fig. 10　Feature-path detection using Hough transformation

stripe from the origin, respectively. The intensity in Hough space corresponds to the number of projected pixels (Fig.9). A maximum peak (θ_{max}, r_{max}) is obtained in Hough space. θ_{max} is the slope angle of the strongest feature path.

3. 1. 4　Plotting Slope-Angle Curve

The θ_{max} obtained from Hough transformation of the stripe ind (θ_{ind}) is the slope angle of the extracted feature path.

A graph plotting the slope angle, θ_{ind}, in the time direction is shown in Fig.11, x and y axis represent stripes index and the slope angle (θ_{ind} (degree)), respectively. If the maximum intensity in Hough space is lower than a predefined threshold, we decide that there is no feature in the stripe. The threshold is calculated as $W_{seg} \times 0.6$, where W_{seg} is the stripe width. After the edge detection of EPIs, a few features of street-parking vehicles are appeared in the binary image. If a feature path is not detected in the stripe, the value of θ_{ind} is changed into the value of θ in the nearest stripe having a feature path. The depth (D) corresponding to the slope of the detected feature path is calculated by the following equation.

$$D = \frac{V \times P}{-m \times f \times \tan\frac{\varphi}{2}} \quad ,$$

where the camera moving speed (the speed of the measurement vehicle) is V (m/s), the pixel number of a scanning line is P (pixels), the angle field of the camera is φ (degree), the line-scan frequency of the camera is f (Hz), the slope of a feature path in the EPI is $m\,(< 0)$.

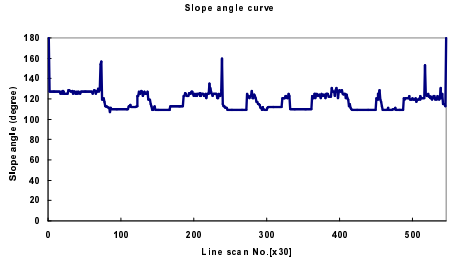

図 11　傾き角度曲線
Fig. 11　slope-angle curve

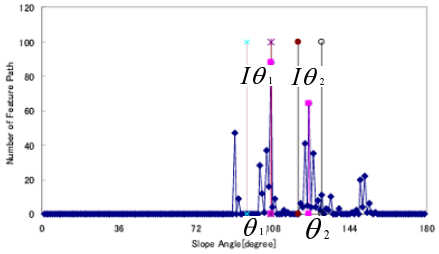

(a) Slope-angle histogram

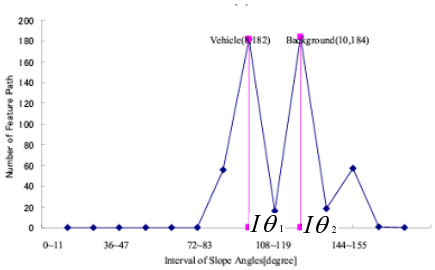

(b) Intervals of slope angle

図 12　特徴直線の傾き角度の閾値
Fig. 12　Threshold of slope angle of feature path

3. 2 Detection of Street-Parking Vehicle from Slope-Angle Curve

Threshold of slope-angle and vehicle length are used for the analysis of slope-angle curve and the decision of the existence of street-parking vehicles.

3. 2. 1　Threshold on Slope-Angle Curve

The depth (D) is proportional to the slope m of the feature path in the EPI. If the slope angle of the feature path ϕ is lower than a threshold, the feature point may belong to the street-parking vehicle and is defined as a candidate for the street-parking vehicle. The threshold value of the slope angle (ϕ_{th}) is determined by experiments. In this paper, it was set at $\theta_{th} = \phi_{th} - 90$ (degree). Fig.12 (a) shows an example of a θ histogram. We divide the histogram along the horizontal axis into a few intervals by a fixed number and calculate the number of feature paths on each intervals

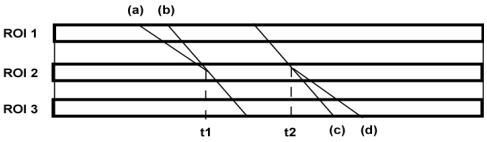

(a) ROIs in EPI

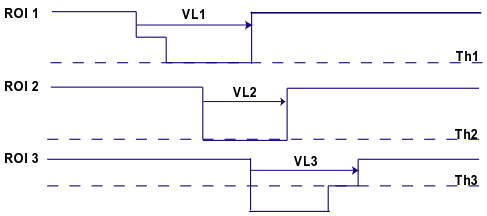

(b) Vehicle lengths in each ROI

図 13　処理領域による車両のピクセル長さ
Fig. 13　ROIs and their corresponding vehicle lengths

(see Fig.12 (b)). Fig.12 (b) shows that there are a few local maximums in the histogram. The slope angles corresponding to the first and second local maximum are defined as the interval of street-parking vehicle's slope angle $I\theta_1$, and background's slope angle $I\theta_2$, respectively. As shown in Fig.12, the slope angle θ_1 and the slope angle θ_2 corresponding to the maximum values in the interval of $I\theta_1$ and $I\theta_2$ are obtained. The average of θ_1 and θ_2 is defined as the threshold value of slope angle (θ_{th}).

3. 2. 2　Vehicle Length

Feature points on the street-parking vehicle draw feature paths on an EPI. The length in time direction is proportional to and can be used in place of a vehicle length (VL (pixels)).

Fig.13 clearly shows how the selection of ROI affects the estimated vehicle length. In the three cases (Fig.13 (b)), the VL_2 is the most appropriable value for vehicle length (see Fig.4); VL_1 and VL_3 is larger than VL_2. The vehicle length is determined by the following equation.

$$VL = \frac{f \times L}{V} \quad ,$$

where L is the length of vehicle (m). VL_{th} (pixels) is calculated from the actual length of the shortest vehicle (L_{min}).

3. 2. 3　Analysis of Slope-Angle Curve

The following pseudocode shows the analysis for θ_{ind}:

$if(\theta_{ind} < \theta_{th}\ AND\ \theta_{ind-1} < \theta_{th})$

　　$VL+ = d;$

$else\ if(VL > VL_{th}\ AND\ \theta_{ind-1} < \theta_{th})$

{

　　A vehicle is detected;

　　$VL = d;$

}

(a) Top ROI

(b) Middle ROI

(c) Bottom ROI

(d) Logical OR of top and bottom ROIs

図 14　上，中，下領域の論理和
Fig. 14　Logical OR of top, middle and bottom regions

$ind++;$

If θ_{ind} and θ_{ind-1} is lower than θ_{th}, the stripe#ind may belong to a street-parking vehicle and a stripe length (d (pixels)) is added to the vehicle pixel length VL. If the θ is larger ($\theta < \theta_{th}$), the VL will be analyzed. If the $VL > VL_{th}$ and $\theta_{ind-1} < \theta_{th}$, a street-parking vehicle is detected, and the VL is set to d in time direction.

3. 2. 4　Measurement for Solving Saturation Problem

If the light, reflected by a car surface enters into the camera lens, the CCD elements will be saturated. This results in a non-feature region in an EPI. The saturation by the reflected light is commonly found in the center of the scan line. To reduce the effect of saturation for improving the reliability, we incorporate the extracted results from 3 ROIs, top, middle and bottom ROI. Fig.14 illustrates how to incorporates the extraction results of top, middle and bottom ROIs. The results from the top, middle and bottom ROIs are bunched together by logical "OR" operator.

4. Region-Based Method

In this section, the detection of street-parking vehicles by region segmentation is described. As shown in the block diagram in Fig.15, the region-based method contains two main steps: morphology processing and template matching.

4. 1　Morphology Processing

This step consists of binarization and morphology processing using opening and colosing operater.

4. 1. 1　Binarization

Binarization processing and Canny algorithm are applied in an EPI for obtaining the feature information of objects.

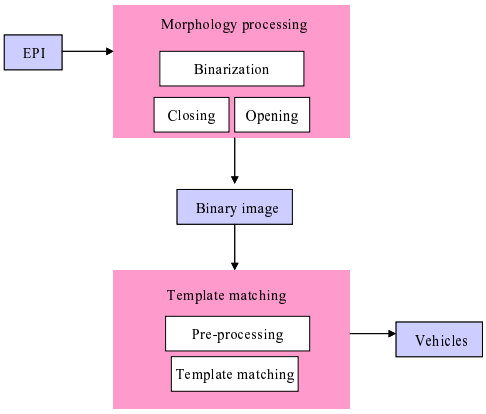

図 15　領域分割法のブロックダイアグラム
Fig. 15　Block diagram of region-based method

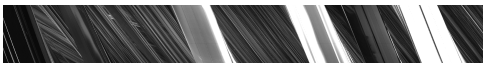

図 16　取得した EPI
Fig. 16　Sample EPI

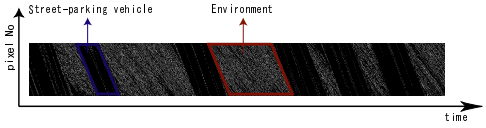

図 17　EPI の 2 値化画像
Fig. 17　Binary image of EPI in Fig.16

Because the background in an EPI has the complex texture, a number of edges are detected in the background. On the other hand, the foreground (vehicle) has only a little texture; thus, there are only few edges detected in the foreground. Binarizing the output of the Canny edge detector results in white and black regions mostly from background and foreground objects, respectively. The regions with many white pixels are the regions of environment because they contain many features. The regions with many black pixels are the regions of vehicles because of their lack of features. Fig.16 and Fig.17 shows a sample of EPI and its corresponding image after binarization.

4. 1. 2　Morphology Processing

Morphology processing [7] is used for separating street-parking vehicles and background regions. In this paper, we used a 3×3 structuring element. First, the closing operator is applied 10 times for connecting the pixels in same background region. Then, the opening operator is applied 10 times for removing small noises in vehicles regions. Fig.18 shows the result, after closing and opening operators are applied to the binary image in Fig.17.

4. 2　Template Matching

This step consists of pre-processing and template matching.

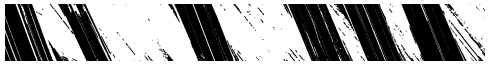

(a) Binary image after closing processing

(b) Binary image after opening processing

図 18　モルフォロジー処理結果
Fig. 18　Morphology processing results

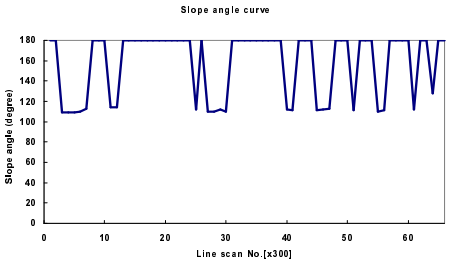

図 19　モルフォロジー処理後求めた奥行き曲線
Fig. 19　The slope-angle curve of Fig.18 (b)

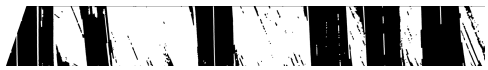

図 20　モルフォロジー処理画像のピクセルシフト結果
Fig. 20　The shifted morphology processed image

4. 2. 1　Pre-Processing

We used template matching for obtaining the regions representing street-parking vehicles. The region of street-parking vehicles has a parallelogramed shape. The following pre-processing is applied for converting parallelograms to rectangles.

Pre-processing:

- Calculation of slope angle using four steps processing described in Section 3.1.

In the slope-angle curve shown in Fig.19, the smallest angle is the approximated slope angle for the feature path of the street-parking vehicle.

- Shift the morphology processed image (Fig.18 (b)) for $\theta_{min} - 90$ degree in the time direction (Fig.20).

A pixel, P_{ind} (ind is the pixel index in the scan line), is shifted by $ind \times tan(\theta_{min} - 90)$ pixels in the time direction.

4. 2. 2　Template Matching

For template images, we used black rectangles. The height of a rectangle is the number of the pixels on one scanning line. The matching result depends on the width of the template image. The matching rate and detected vehicle lengths for 25 and 70 pixels widths are shown in Fig.21 and 22, respectively.

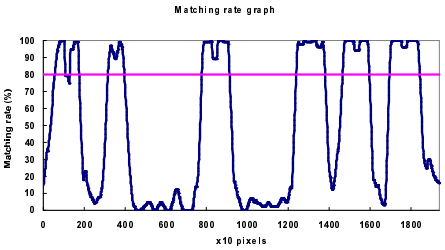

(a) Matching rate

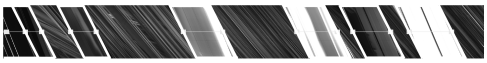

(b) Vehicle length

図 21　25 ピクセルのテンプレートのマッチング結果
Fig. 21　25 pixels width template matching result

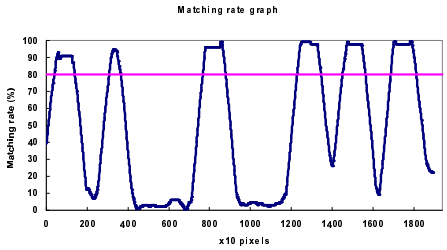

(a) Matching rate

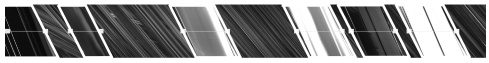

(b) Vehicle length

図 22　70 ピクセルのテンプレートのマッチング結果
Fig. 22　70 pixels width template matching result

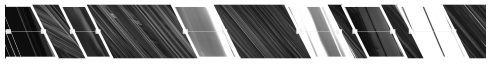

図 23　二つの幅のテンプレートでマッチングした結果
Fig. 23　Two templates with different widths are used

It is important to appropriately set the width of the template. If the width of the template is too short, the parking vehicles may be overcounted: one vehicle is detected as two or more vehicles (see the first street-parking vehicle in Fig.21). If the width is too long, the detected vehicle length is inaccurate and some vehicles may not be detected. In Fig.22, the detected vehicle length is longer than the actual length. For obtaining the correct number and vehicle length of street-parking vehicles, we use the width of two templates for matching and fuse the two results together.

First, a template with the length of approximated threshold of vehicle length, VL_{th}, is used for detecting street-parking vehicles.

After that, a template with shorter length is used to determine the vehicle length.

The result of the two-template processing is shown in Fig.23.

5. Fusion of Edge- and Region- Based Methods

The edge- and region- based methods are fused for the more robust detection system. The vehicle-segment sequences 1 and 2 are the results of edge-based method and region-based method, respectively. The two sequences are processed by logical operators as follows;

1) Logical "AND" operator is applied to vehicle-segments 1 and 2. The resulting segments are defined as "AND-sequence". In the "AND-sequence", each segment is detected as an individual vehicle, regardless of its length.

2) Logical "XOR" operator is applied to vehicle-segments 1 and 2. The resulting segments are defined as "XOR-sequence". In the "XOR-sequence", segments longer than VL_{th} are detected as vehicles.

The number of vehicles detected from the AND and XOR sequences is the number of vehicles detected in the fusion phase.

Tipical three cases are explained in Fig.24.

- Case 1: The region detected vehicle using region-based method includes the region detected vehicle using edge-based method ($F_1 < F_2 < T_2 < T_1$) . If $F_2 - F_1 > VL_{th}$, a vehicle is detected from F_1 to F_2. A vehicle is detected from F_2 to T_2. If $T_1 - T_2 > VL_{th}$, a vehicle is detected from T_2 to T_1.
- Case 2: There is an overlapped region of detected vehicle using edge-based method and region-based method ($F_4 < F_3 < T_4 < T_3$) . If $F_3 - F_4 > VL_{th}$ (VL_{th} is the threshold vehicle length detailed before), a vehicle is detected from F_4 to F_3. A vehicle is detected from F_3 to T_4. If $T_3 - T_4 > VL_{th}$, a vehicle is detected from T_4 to T_3.
- Case 3: A vehicle detected in the region from F_5 to T_5 using edge-based method, but no a part of a vehicle is detected in the region using region-based method. In that case, we decide that there is a vehicle detected from F_1 to T_1. (logical OR)

6. Experimental Results

We conducted experiments by driving our measurement vehicle along "Housya Route 23" road (the interval between "Yoyogi Koen Koban Mae" intersection and "Shibuya-ku Jinen-chou" intersection). The camera was operated at high and low line-scan frequency, 1.8kHz and 200Hz.

The results at high and low line-scan frequency are shown

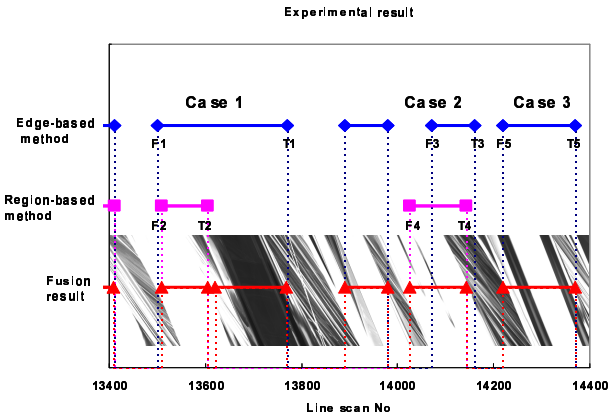

図 24　二つの手法を融合した結果
Fig. 24　Experimental result fusing two methods

表 1　周波数 1.8kHz の場合の結果
Table 1　Result in the frequency of 1.8kHz

	TruePositive	FalsePositive	FalseNegative
Edge-based method	78	1	0
Region-based method	77	4	1

表 2　周波数 200Hz の場合の結果
Table 2　Result in the frequency of 200Hz

	TruePositive	FalsePositive	FalseNegative
Edge-based method	89	0	10
Region-based method	54	0	45

表 3　融 合 結 果
Table 3　Fusion result

	TruePositive	FalsePositive	FalseNegative
Fusion result	95	2	4

in Table 1 and Table 2, respectively. **TruePositive** and **FalsePositive** are the number of vehicles correctly detected and the number of background regions detected as vehicles, respectively. **FalseNegative** is the number of vehicles undetected. The detection rate was calculated as $\frac{TruePositive}{TruePositive+FalseNegative}$. At the high line-scan frequency, 1.8kHz, the detection rates of edge- and region- based methods were 78/78 (100%) and 77/78 (98.7%), respectively. At the low lin-scan frequency, 200Hz, the detection rates of edge- and region- based methods were 89/99 (89.9%) and 54/99 (54.5%), respectively. From the experiment, we can conclude that the detection rate is affected by the lin-scan frequency. The detection rate is better at the high frequency than at the low frequency.

The fusion result in the low frequency, 200Hz, is shown in Table 3. The detection rate was improved to 95/99 (96.0%).

7. Conclusions

We proposed the detection method for street-parking vehicles: the method is based on the EPI analysis. The detection method fuses the edge- and region- based algorithms. The edge-based algorithm uses depth information from feature paths detected in EPIs. The region-based algorithm uses texture information from the morphology processed edges of EPIs. From our experiments, the detection rate obtained by fusing two algorithms reached 96%, even at the low frequency 200Hz.

Our future work is classification of street-parking vehicles from panoramic and epipolar-plane images obtained by using horizontal- and vertical-scanning line-scan cameras.

Acknowledgement

This work was in part supported by ITS division, the Research Center for Advanced Information Technology, the National Institute for Land and Infrastructure Management (NILIM), the Ministry of Land, Infrastructure and Transport (MLIT), Japan.

References

[1] S.Ono, M.Kagesawa and K.Ikeuchi, "Parking-Vehicle Detection System by Using Laser Range Sensor Mounted on a Probe Car," *Proc. IEEE Intelligent Vehicle Symp.*, 2002.

[2] R.C.Bolles, H.H.Baker and D.H.Marimont, "Epipolar-Plane Image Analysis: An Approach to Determining Structure from Motion," *Int'l J. Compute Vision*, Vol.1, pp.7-55, 1987.

[3] H. Baker and R.C.Bolles, "Generalizing Epipolar Plane Image Analysis on the Spatiotemporal Surface," *Int'l J. Computer Vision*, Vol.3, pp.33-49, 1989.

[4] M. Yamamoto, "Determining Three-Dimensional Structure from Image Sequences given by Horizontal and Vertical Moving Camera," *IECE Trans.*, Vol. J69-D, No.11, pp.1631-1638, 1986 (in Japanese).

[5] J. Canny, "A Computational Approach to Edge Detection," *IEEE Trans. Pattern Analysis and Machine Intelligence*, Vol.8, No.6, pp.679-698, 1986.

[6] P.V.C. Hough, "Machine Analysis of Bubble Chamber Pictures," *Proc. Int'l Conf. High Energy Accelerators and Instrumentation*, pp.536-554, 1959.

[7] J.Serra, "Image Analysis and Mathematical Morphology," *Academic Press*, 1982.

[8] P.Wang, K.Ikeuchi and M.Sakauchi, "3D Line's Extraction From 2D Spatio-temporal Image Created by Sine Slit," *Proc. Asian Conf. Computer Vision*, pp.408-415, 1998.

[9] S.Sakuma, Y.Takahashi, A.Shio and S.Ohtsuka, "Vehicle Counter System Using Panoramic Images," *IEICE Trans. Information and Systems*, Vol.J85-D, No.8, pp.1361-1364, 2002.